Journal of Inflammation Research

Dovepress
Taylor & Francis Group

Open Access Full Text Article

ORIGINAL RESEARCH

Reduced Thioredoxin Regulates IL-1β Secretion via NLRP3 of IL-1β+ Alveolar Macrophages in COPD

Lueli Wang[1,*], Rui Shi[1,*], Zhaoliang Li[1], Ruoqiu Ma[1], Chongyu Wang[1,2], Changli Xu[1], Rong Guo[1], Chuang Xiao[1], Xiaohua Du[3], Weimin Yang[1]

[1]Yunnan Key Laboratory of Pharmacology for Natural Products, Kunming Medical University, Kunming, People's Republic of China; [2]Pharmacy Department, The First People's Hospital of Zhaotong, Zhaotong, People's Republic of China; [3]Geriatric Respiratory Department, First Affiliated Hospital of Kunming Medical University, Kunming, People's Republic of China

*These authors contributed equally to this work

Correspondence: Xiaohua Du, Geriatric Respiratory Department, First Affiliated Hospital of Kunming Medical University, Kunming, People's Republic of China, Email dxiaohuabs@126.com; Weimin Yang, Yunnan Key Laboratory of Pharmacology for Natural Products, Kunming Medical University, Chunrong West Road, Kunming, 650500, People's Republic of China, Email yangweimin@kmmu.edu.cn

Objective: Chronic obstructive pulmonary disease (COPD) is a disease with a complex etiology. The secretion of inflammatory factors, such as IL-1β and oxidative stress, plays an important role in the pathogenesis of COPD. The aim of this paper is to investigate the changes in the redox protein thioredoxin (TRX) in COPD and the role TRX plays in IL-1β release.

Methods: We analyzed data from single-cell RNA sequencing (scRNA-seq) of COPD lung tissue in the GEO database. Changes in TRX expression levels and activity were assessed by protein activity analysis of alveolar macrophages(AM). Using Monocle2 and molecular dynamics(MD) to analyze which pathways through TRX achieves regulation of the inflammatory response. The analytical results were subsequently validated by constructing vivo and vitro models.

Results: AM that specifically synthesize IL-1β were identified by scRNA-seq. No change in TRX expression levels and decreased protein antioxidant activity in IL-1β+ AM with COPD. We confirmed an increase in oxidized TRX (oxTRX) and a decrease in reduced TRX (reTRX) in COPD mouse model and THP-1 cell model. The decrease in reTRX was accompanied by the upregulation of NLRP3 activity, which played a catalytic role in the synthesis of IL-1β in this subgroup. This was subsequently confirmed in a cigarette smoke-induced THP-1 cell model. A decrease in reTRX level accompanied by an upregulation of NLRP3 activity, which plays a facilitating role in the synthesis of IL-1β. We determined that reTRX reduction was followed by depolymerization of thioredoxin-interacting protein (TXNIP) through MD and immune co-precipitation (CO-IP). Then TNXIP interacted with NLRP3 and up-regulate NLRP3 activity, which in turn promoted IL-1β release.

Conclusion: Our study shows that the reTRX is abnormally altered in COPD and leads to the upregulation of NLRP3 activity in AM to enhance IL-1β production.

Keywords: chronic obstructive pulmonary disease, single-cell RNA sequencing, alveolar macrophages, thioredoxin, inflammations

Introduction

Chronic obstructive pulmonary disease (COPD) is a common chronic respiratory disease and a serious health and economic burden in many countries around the world. The pathological changes of COPD are characterized by chronic inflammatory, small airway damage and abnormal remodeling. The pathogenesis of COPD include the abnormal presence of an inflammatory response, oxidative-antioxidant imbalance, and protease-antiprotease imbalance.[1] These factors do not exist independently, but rather cause and promote the progression of the disease. For example, after inflammatory cells are activated, they promote reactive oxygen species (ROS), which induces an oxidative-antioxidant imbalance. Conversely, excessive ROS can also promote abnormal activation of inflammatory cells.[2,3]

Received: 18 December 2024
Accepted: 26 June 2025
Published: 30 June 2025

The thioredoxin system is an important member of the human antioxidant system, consisting of thioredoxin, thioredoxin reductase and NADPH. Thioredoxin includes two subtypes. Subtype 2 (TRX2) is mainly located in mitochondria and the nucleus, where it performs antioxidant or transcriptional regulatory functions.[3] Thioredoxin Subtype 1 (TRX) is mainly located in the cytoplasm of the cell and is encoded by the TXN gene.[4,5] It performs functions such as antioxidant protection or regulation of immune and inflammatory responses. TRX maintains the reduced state and natural conformation of proteins by opening the disulfide bonds in the proteins. Then thioredoxin reductase and NADPH reduce the oxidized TRX(oxTRX) to the reduced TRX(reTRX) and enter the next round of reducing proteins.[6,7] TRX has an interactive protein called thioredoxin-interacting protein (TXNIP). When TRX is in a reduced state, TRX and TXNIP are in a bound state. When TRX is oxidized, the TXNIP is uncoupled from oxTRX. The dissociated state of TXNIP regulates other proteins to achieve crosstalk between oxidative stress and other physiological functions. Current research has confirmed that increasing the TRX content in lung tissue can effectively improve oxidative stress and immune inflammatory responses, but the role of TRX in the pathological mechanism of COPD is still unclear.[8]

The NOD-like receptor pyrin domain-containing protein (NLRP) family is a key member of the NOD-like receptor (NLR) family and is mainly involved in innate immune responses and inflammatory responses. The NLRP subfamily, upon activation, recruits and activates caspase-1, which subsequently leads to the production and release of mature IL-1β (Encoding gene: IL1B).[9] The NLRP family consists of a variety of proteins, among which NLRP3 is the subtype that has been studied most in COPD disease. NLRP3 can mediate the production and release of IL-1β by many immune and inflammatory cells, thereby influencing with the progression of COPD. Our previous research confirmed that NLRP3 activity is increased in COPD and leads to increased IL-1β release, and that intervention with NLRP3 activity through chemical compounds can improve the progression of COPD in mouse models.[10] TRX can regulate oxidative stress on the inflammatory response through regulation of the NLRP family, thereby inhibiting IL-1β release in downstream pathways.[11] For example, TXN is an endogenous ligand for NLRP1, which can inhibit NLRP1 activity by binding to NLRP1.[12] For the regulation of NLRP3, TRX can directly inhibit NLRP3 activity without the involvement of other proteins.[8] TRX can also regulate NLRP3 activity by dissociating the TXNIP protein and then TXNIP binding to NLRP3.[13]

Single-cell RNA sequence (scRNA-seq) is a cell-level RNA sequencing technique. scRNA-seq studies in COPD have revealed the roles played by epithelial cells, lymphocytes, dendritic cells, and granulocytes in tissue damage repair and immune inflammatory responses. Here, we identified IL-1β-secreting AMs in the scRNA-seq data of lung tissue from COPD patients. Analysis of the mRNA levels and protein activity prediction of IL-1β+ AMs suggest that under disease conditions, the mRNA levels of TRX in IL-1β+ AMs remain unchanged, while protein activity decreases. In vivo and in vitro experiments confirmed that reTRX is reduced, oxTRX is increased, and antioxidant activity is reduced under disease conditions. Through pseudo-temporal analysis and in vitro experiments, it was confirmed that TXN promotes the secretion of IL-1β through NLRP3. Through molecular dynamics simulation, immuno co-precipitation (CO-IP) and in vitro experiments, it was predicted that TRX does not directly interact with NLRP3, but indirectly regulates NLRP3 through TXNIP. This study clarifies the role of TRX in COPD and provides a pharmacological basis for TRX as a drug target for the treatment of COPD.

Material and Methods

Data Acquisition and scRNA-Seq Analysis

The data used was from the GEO database of the public database. The SRR files were downloaded from this dataset, which included lung tissue from 6 patients with COPD and 6 healthy people. The barcode, feature, and count files were used as input files for the Seurat V4.0 software.[14] R package Harmony was used to remove batch effects between samples.[15] Seurat software was used to perform quality control on the data. nCount was set to greater than 300 to remove empty droplets or dead cells during sequencing. nFeature was set to less than 2000 to remove double cells, and the mitochondrial gene ratio was set to greater than 20% to remove dead cells. scDBlFinder was used to remove double cells.[16] The data was successively processed by data normalization, finding the nearest distance, dimensionality reduction, and clustering. The cell subpopulations were annotated according to the marker genes provided in previous

literature. Then, the differential genes were analyzed using the findmarker function, and the enrichment analysis of the differential genes was performed using the R package ClusterProfiler.[17] Visualization was performed using ggplot2.

Protein Activity Analysis Using metaVIPER

Extract the AM expression matrix from the Seurat object, use the ARACNe-AP software to generate a protein regulatory network. Then use the metaVIPER[18] to generate a protein activity matrix for AM. Differentially expressed genes were analyzed using a *t*-test, and an enrichment analysis of differentially expressed genes was performed using the R package ClusterProfiler. Visualization was performed using ggplot2.

Monocle2 for Pseudotime Analysis

Using the R package Monocle2,[19] a pseudotime analysis object was constructed from the Seurat object. After sequencing the AM, the gene expression and protein activity of the sequenced cells were analyzed. Visualization was performed using ggplot2.

Reagent Preparation

Add 1640 medium (BI) to a glass gas-washing flask and prepare CSE by blowing cigarette smoke into the glass gas-washing flask at a ratio of 1 mL medium to 1 cigarette. Filter the CSE through a 0.22 μm filter to sterilize it, aliquot it and store it at −20 °C for later use.

Place TRX dry powder (MCE, Cat No.HY-P73431A) in a 4°C oxygen enriched environment for 1 month. Identify the oxTRX by non-denaturing electrophoresis and freeze it at −20°C after all TRX is oxidized.

The reagent contains Guanidine·HCl (6 M), EDTA (3 mM), Tris·HCl (50 mM), IAA (100 mM), 0.5 mL Triton X-100 (0.5%), and the pH is adjusted to 8.3. It is freshly prepared before use.

Animal Model Construction

We used cigarette smoke exposure to model mouse based on previous studies.[20] C57/BL mouse were purchased from the Kunming Medical University Laboratory Animal Center. Animal experiments were approved by the Kunming Medical University Ethics Committee. At week 0, intratracheal instillation of LPS (0.5 mg/kg) was performed to establish the model. Cigarette smoke exposure (1 cigarette/mouse/day) was performed from week 1 to week 16. On the first day of week 16, the second intratracheal instillation of LPS was performed. All mouse were euthanized and the lung were recovered on the first day of week 17.

Immunofluorescence (IF)

The pathological sections were successively baked, dewaxed, hydrated, and then antigen-repaired using the citrate method. Blocking and permeabilization were performed with PBS containing 5% goat serum and 0.3% Triton X-100. The primary antibodies (Anti-Cd68 (ProteinTech, Cat No.3A97A), Anti-Cd206 (ProteinTech Cat No.2A6A10), Anti-Marco (ABclonal, Cat No.A10048), Anti-TRX (MCE, Cat No.HY-P80912)) were incubated overnight at 4°C. Incubate with secondary antibody conjugated with fluorescent dye at room temperature for 1h in the dark, and stain with DAPI. Take pictures using a Nikon upright microscope.

Cell Culture

Use the THP-1 cell line, purchased from HaiXing Biosciences, and the cell line has been STR identified before use. Use 1640 medium (BI) containing 10% FBS (BI) to culture the cells in a semi-exchange liquid medium.

Cell Model Establishment

THP-1 cells were induced with PMA (MCE, Cat No.HY-18739) for 24 hours after attachment, and then LPS (Sigma, Cat No.297–473-0) was added to induce THP-1 cell differentiation. After that, a certain concentration of cigarette smoke extract was added to stimulate the cells for 48 hours. The medium in the well plate was replaced with medium containing LPS (200 ng/mL) and TRX, PX12 (MCE, Cat No.HY-13734) and MCC950 (TargetMol, Cat No.CP-456773) according

to the group for incubation for 6 hours, and then a concentration gradient of ATP was added for incubation for 1 hour. The supernatant was collected for testing.

Protein Extraction and Immunoblotting

Denatured Sample Preparation and Denaturing Electrophoresis

To detect the total protein level, denaturing electrophoresis was performed using SDS-PAGE. Protein extraction was performed using RIPA lysis buffer. Use electrophoresis to separate the protein. Then transfer the protein to PVDF membrane (Macklin). The PVDF membrane was incubated with primary antibody (Anti-TRX (MCE, Cat No.HY-P80912), Anti-β actin (ProteinTech, Cat No.2D4H5)), secondary antibody. The blot signal was collected using an ultra-sensitive developer (GE AI600).

To detect the reTRX and ox TRX protein level, non-denaturing electrophoresis was performed using NATIVE-PAGE. Protein extraction was performed using G-lysis buffer. Use electrophoresis to separate the protein. Then transfer the protein to PVDF membrane (Macklin). The PVDF membrane was incubated with primary antibody (Anti-TRX (MCE, Cat No.HY-P80912)), secondary antibody. The blot signal was collected using an ultra-sensitive developer (GE AI600).

Dot Blot of Cell Supernatant

After collecting the cell culture supernatant, the supernatant was quantified and at a uniform concentration. Then the sample was spotted onto the activated PVDF. The PVDF membrane was incubated with primary antibody (Anti-IL-1β (CST, Cat No.D3U3E)) and secondary antibody in sequence. The signal was collected using a supersensitive developer (GE AI600).

Active Protein Extraction and Insulin Precipitation Experiment

Protein extraction was performed using active protein extraction reagent (Beyotime). The reaction system was prepared using PBS. The concentration of insulin (MCE, Cat No.11070–73-8) in the system was 0.13 mmol/L, and the activity protein was 4 μg/mL. Then, dithiothreitol (DTT) was added to a final concentration of 1 mmol/L to start the reaction. The absorbance (OD) was measured every 1 min at 600 nm to plot the reaction curve.

Immuno Co-Precipitation

The cells were lysed with NP-40 lysis buffer (Beyotime). According to the operating procedures of the kit (Beyotime), a ProteinA/G magnetic bead-antibody complex (Anti-NLRP3 (ProteinTech, Cat No.3H1A7)) was prepared, and the ProteinA/G magnetic bead-antibody complex was mixed with the protein solution and incubated overnight. The complex was depolymerized using an SDS loading buffer containing β-mercaptoethanol. The sample was subjected to subsequent SDS-PAGE detection (Anti-NLRP3 (MCE, Cat No)., Anti-TRX (MCE, Cat No.HY-P80912), Anti-TXNIP (ABclonal, Cat No.A24289), Anti-β actin (ProteinTech, Cat No.2D4H5)).

Molecular Dynamics Simulation

Download the three-dimensional structures of TRX, TNXIP, NLRP3 proteins and ATP from the PDB database. Upload the protein structure file to the Charmm-Gui website,[21] and use the Charmm36 force field to generate the Gromacs input software. The input file was imported into the Gromacs (v2023.3) software,[22] and after energy minimization and system pre-equilibration, the finished product was subjected to a kinetic simulation. The simulation results were used to calculate the root mean square deviation (RMSD) using Gromacs and the binding free energy using the gmx_mmpbsa script.[23] The results were visualized using PyMOL and ggplot2.

Statistical Analysis

Statistical analysis was performed using GraphPad Prism 8. Continuous variables are expressed as mean ± SEM. The Shapiro–Wilk (S-W) test was used to verify the normality of the data. For pairwise comparisons, data that conformed to normal distribution were analyzed using the *t*-test, and data that did not conform to normal distribution were analyzed using the Mann-Whitney *U*-test. For multiple group comparisons, data that conforms to a normal distribution is analyzed

using one-way ANOVA, and data that does not conform to a normal distribution is analyzed using the Kruskal–Wallis (K-W) test. For fitting analysis, data that conforms to a linear relationship is fitted using a linear regression equation, and data that does not conform to a linear relationship is fitted using a 4-factor Logistics regression equation to calculate the EC50 value. Visualization was performed using ggplot2.

Results

scRNA-Seq results Suggest an Increased Percentage of AM in COPD Lung Tissue

We retrieved the GSE173896 dataset, which samples healthy and COPD patients' lung tissues for single-cell sequencing using the 10× platform. Six cases were downloaded from the control group and six cases from the COPD group. Preliminary quality control and expression quantification of fastq data were performed using cellranger software, and a total of 43,575 cells were obtained. Afterward, we performed quality control and removal of double cells, and obtained 37,268 cells. Based on the above data, we performed downscaling and subclustering (Figure 1A).Then annotated each subcluster, including ciliated cells, type II alveolar epithelial cells, type I alveolar epithelial cells, Club cells, smooth muscle cells, T lymphocytes (T cell), natural killer cells (NK), B lymphocytes (B cell), plasma cells, mast cells, fibroblasts, endothelial cells, and myeloid cells. The marker genes used for the annotation of each subcluster referenced databases and previous literature with good specificity (Figure 1C). The accuracy of the subcluster annotations was further confirmed by extracting the top 200 highly variable genes of the subpopulation for enrichment analysis. For example, T cell highly variable genes were enriched to T cell activation, NK cell were enriched to cell killing, and macrophages were enriched to regulate lymphocyte activation and modulate immune response. Myeloid subpopulations could be further identified as AM, interstitial macrophages (IM), classical dendritic cells 1 (cDC1), classical dendritic cells 2 (cDC2), plasmacytoid dendritic cells (pDC), and mononuclear-like dendritic cells (MonoDC).

We counted the cell occupancy in control and COPD (Figure 1B), and it was seen that immune cells, except NK cells, were up-regulated in the COPD group. Endothelial and stromal cells were down-regulated in the COPD group, and epithelial cells were up-regulated in the COPD group. Among the myeloid subcluster, AM had the highest percentage and was up-regulated in the COPD group ratio. AM are immune cells residing in the alveolar lumen, derived from monocytes in the bone marrow and matured in lung tissue. They are involved in immune defense and tissue repair

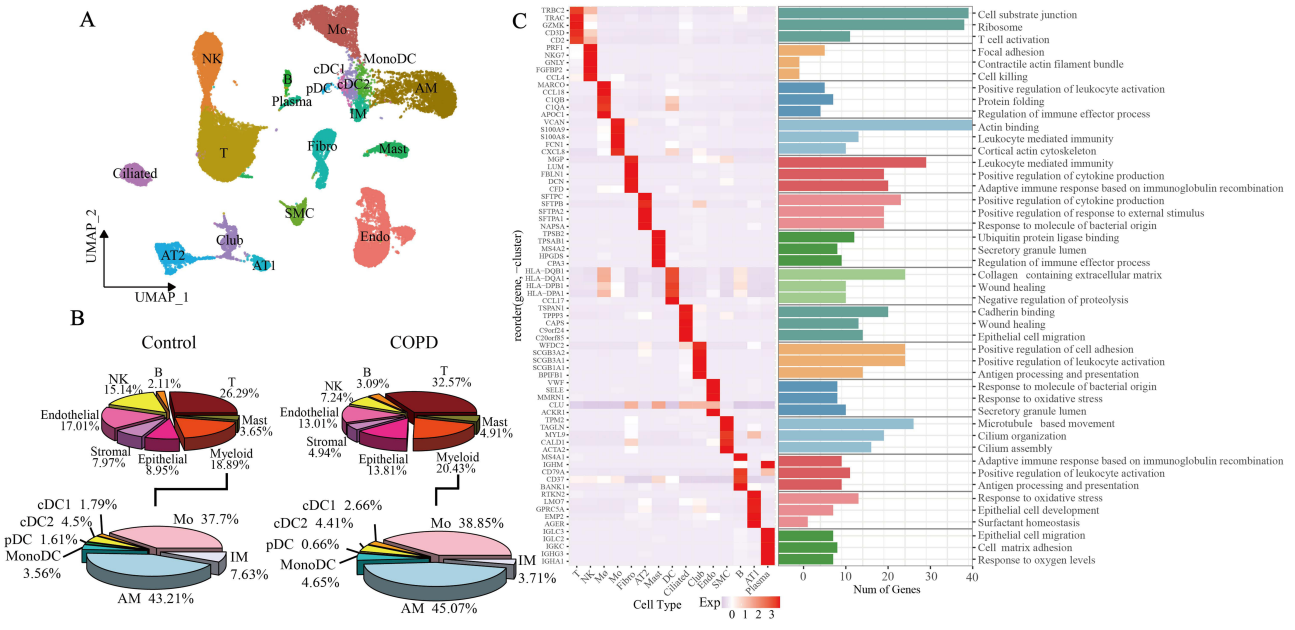

Figure 1 Lung tissue scRNA-seq data cell subclusters. (**A**) UMAP plot showing the cell subclusters identified. (**B**) Pie chart showing the percentage of each cell subcluster and myeloid subcluster in the control and COPD groups. (**C**) Marker gene heatmap and enrichment plot showing the marker genes used to identify the subclusters, and the functions suggested to be exercised by the cellular subclusters based on the marker gene enrichment results.

https://doi.org/10.2147/JIR.S513004

through phagocytosis, antigen presentation, and secretion of various cytokines. In COPD, AM contribute to the inflammatory response through multiple mechanisms. External stimuli such as smoking and environmental pollution activate AM, causing them to release large amounts of pro-inflammatory cytokines such as IL-1β. These cytokines not only contribute directly to airway inflammation and tissue destruction, but also recruit and activate other immune cells, such as neutrophils and T cells, which further exacerbate the inflammatory response.[24,25] We will follow up with further analysis of the AM subcluster.

Decreased Antioxidant Activity of IL-1β+ AM in COPD

We downscale the AM subcluster and we get 3 subclusters. We showed the TOP 5 marker gene for each subcluster in the UMAP plot (Figure 2A). Based on the marker gene, we annotated them as IL1B+ AM, CCL2+ AM and CSDE1+ AM, with 2,275, 644 and 120 cells. By enrichment analysis of the TOP 25 marker gene (Figure 2B), the IL1B+ AM subcluster was enriched for inflammatory responses, cytokines, responses to microorganisms, and responses to reactive oxygen species. The Marker gene had CXCL5 that recruits macrophages and neutrophils.[26] IL1B that is secreted predominantly by AM, and is a key COPD exacerbation cytokines.[27] MCEMP1, LY6E and TREM1 are involved in regulating the abnormal repair and immune-inflammatory response of AM in lung tissues.[28–30] CCL2+ AM subcluster is enriched to leukocytes wandering, chemotaxis, cell activation and involved in immune response, antigen processing and presentation. In marker gene has a large number of chemokines, including CCL2, CCL4L2, CCL3, CCL3L1 and CCL4, which can recruit immune cells through chemokines. For example, CCL2 recruits monocytes, macrophages, dendritic cells, and some T cells.[31] The CSDE1+ AM subcluster is enriched for functions related to DNA transcription, RNA synthesis, and protein translation.

Considering that AM and IL-1β play important roles in COPD, we chose to analyze IL1B+ AM. Differential expression analysis was first performed on the IL-1β+ AM subcluster (Figure 2C), and a total of 177 genes with up-regulated expression and 153 genes with down-regulated expression were obtained in COPD. And the top 10 upregulated genes in the COPD group included CD74, CTSB, CST3, PSAP, XIST, SCGB3A1, SCGB1A1, HLA-DEA1, C1QC, and HLA-DPA1. Which were mainly associated with immune-inflammatory responses. Among them, CD74, HLA-DEA1 and HLA-DPA1 are related to antigen presentation, and the abnormal antigen presentation process may lead to chronic inflammation in lung tissues of patients with COPD.[32] C1QC is a complement component, which is involved in immune response processes such as clearing of pathogens, and previous studies have suggested that the degree of up-regulation in the expression of C1QC is correlated with the severity of the disease.[33] Enrichment analysis of genes showed that up-regulated genes in COPD were enriched for biological behaviors or pathways such as protein degradation and synthesis, immuno-inflammatory processes, and energy metabolism. The top ten down-regulated genes included FAU, RAB11FIP1, TSPO, RPS5, CD9, LDHB, EVL, H3F3A, NDUFS5, and JUND. JUND is a member of the AP-1 family of transcription factors, and deletion of its expression leads to increased inflammation and emphysema.[34] Enrichment analysis of genes showed that down-regulated genes in COPD were enriched for biological behaviors or pathways such as protein synthesis, immune-inflammatory processes, and energy metabolism.

Proteins are the main bearers of life activities. During the process of synthesizing mRNA and directing the translation of proteins, there are many factors that affect the production and activity of the final proteins. scRNA-seq is an assay of mRNA level and does not fully characterize the level of protein activity in the cell. And we used metaVIPER software to analyze the protein activity of IL1B+ AM subcluster, proteins included in the analysis including transcription factors, signaling proteins, and surface markers. After obtaining the protein activity expression matrix, differential analysis of protein activity was performed (Figure 2D). A total of 53 activity up-regulated genes in COPD and 83 activity down-regulated genes in COPD. The top ten up-regulated genes in the COPD group included GRN, SQSTM1, HLA.DQA1, HLA.DPA1, SCGB1A1, CEBPD, RAB7A, HLA.F, HLA.DOA, ATP6V1B2. Among them, GRN, SCGB1A1 affected the COPD disease process by regulating the damage repair and inflammation in lung tissues.[35,36] HLA-DQA1, HLA-DPA1, HLA-F, HLA-DOA contribute to the progression of the inflammatory response in COPD through antigen presentation.[37] SQSTM1 is involved in the regulation of autophagy for the regulation of the macrophage inflammatory response.[38] Enrichment analysis of up-regulated genes enriched for biological behaviors or pathways such as immune-inflammatory response, cell migration and adhesion, and transcriptional regulation. The top ten down-regulated genes in COPD

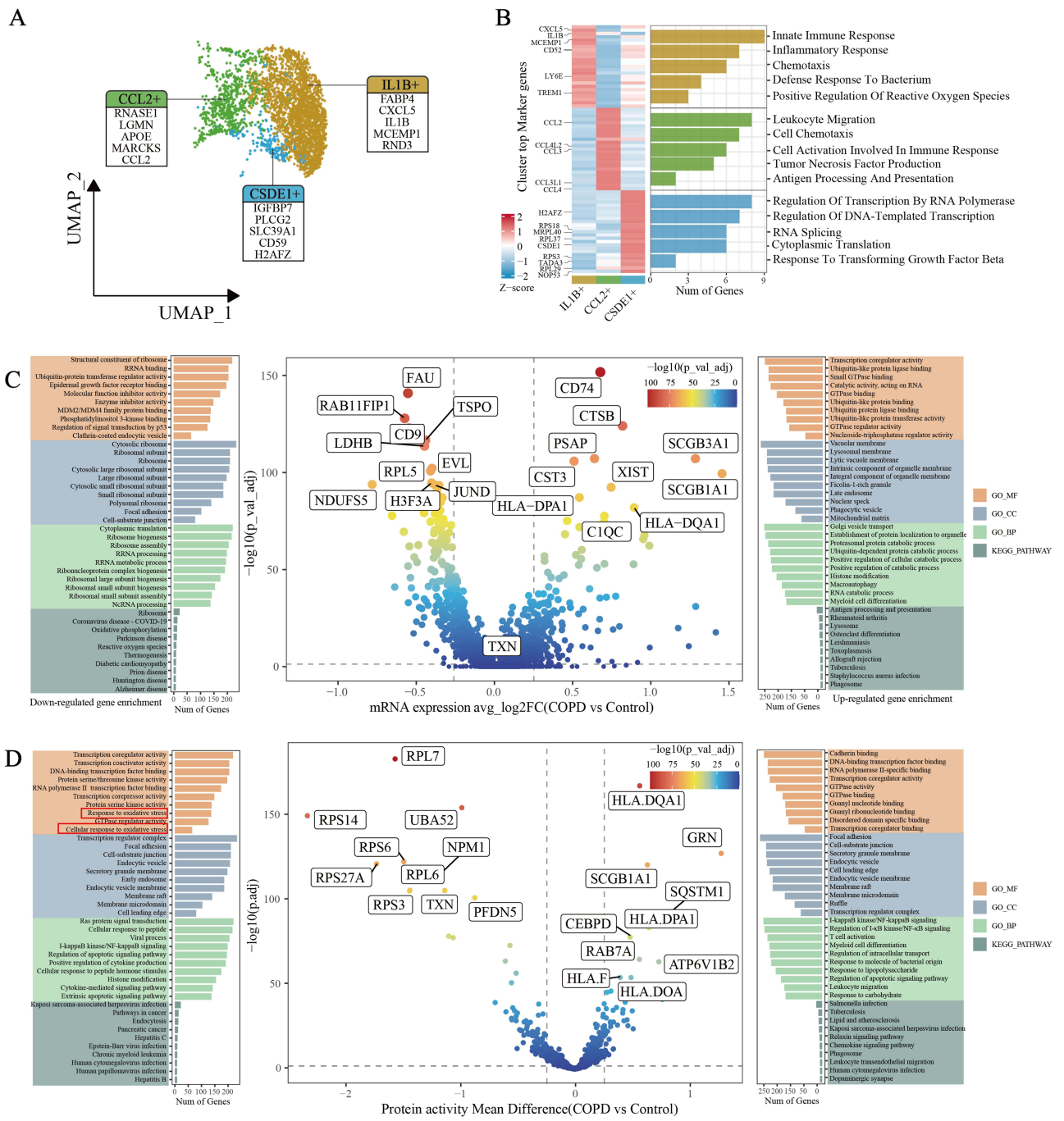

Figure 2 AM downscaling and subclustering, differential genes and differentially active proteins. (**A**) UMP plot Demonstrating further subclusters obtained for AM subcluster, and marker genes used. (**B**) Heatmap highly variable genes of three subclusters of AM, and their GO enrichment results. (**C** and **D**) Volcano plot Differential genes within the IL-1β+ AM obtained from RNA expression matrix and protein activity prediction results, and up- and down-regulated genes enriched to signaling pathways.

included RPL7, RPS14, UBA52, RPS6, NPM1, RPL6, RPS27A, RPS3, TXN, PFDN5. Among them, RPL7, RPS14, RPS6, RPL6, RPS27A, RPS3, UBA52, RPS27A are involved in the process of protein synthesis and degradation.TXN gene encodes thioredoxin(TRX). TRX is an important antioxidant protein, and previous studies have suggested that TRX supplementation improves COPD prognosis.

Comparing the results of differential analysis of mRNA with those of protein activity, we found more similar changes in immune-inflammatory response, protein synthesis degradation, and energy metabolism. Oxidative stress-related genes did not change at the mRNA expression level, whereas they were found in genes that were downregulated at the protein

https://doi.org/10.2147/JIR.S513004

activity level. It seems that the protein activity changes are more compatible with previous studies of COPD pathomechanisms. Among the oxidative stress-related genes with down-regulated protein activity, TRX was most significantly down-regulated, and we further analyzed TRX.

Decreased Antioxidant Activity of TRX in IL1-β+ AM

To understand the distribution of TRX, TRX expression was projected onto a UMAP map (Figure 3A), which showed that TRX was distributed in the lungs mainly in AM, pDCs, and a few ciliated epithelial cells. We performed immunofluorescence co-localization experiments on mouse lung tissues (Figure 3B), which showed good co-localization of TRX protein and alveolar macrophage markers (Cd68, Cd206, Marco). The mRNA expression and protein activity of the IL1-β+ AM subcluster TRX were analyzed (Figure 3C). TRX had the highest mRNA expression in the IL1B+ AM subcluster, followed by CCL2+ AM, and the lowest expression in CSDE1+ AM. There was no difference in expression between healthy and COPD subclusters. The protein activity of TRX was decreased to varying degrees in all three subclusters, IL1B+ AM, CCL2+ AM, and CSDE1+ AM, with the most significant decrease in IL1B+ AM.

To confirm what caused the decrease in TRX activity, we constructed a mouse COPD animal model and a cell model of the THP-1 cell line. TRX activity was assayed (Figure 3D). In the mouse model, the antioxidant capacity of TRX was decreased in the model group compared with the control group. In the cellular model, the antioxidant capacity of TRX gradually decreased with increasing concentrations of CSE. To clarify whether the changes were caused by changes in TRX protein levels or changes in redox status, we examined the total amount of TRX in the model using denaturing

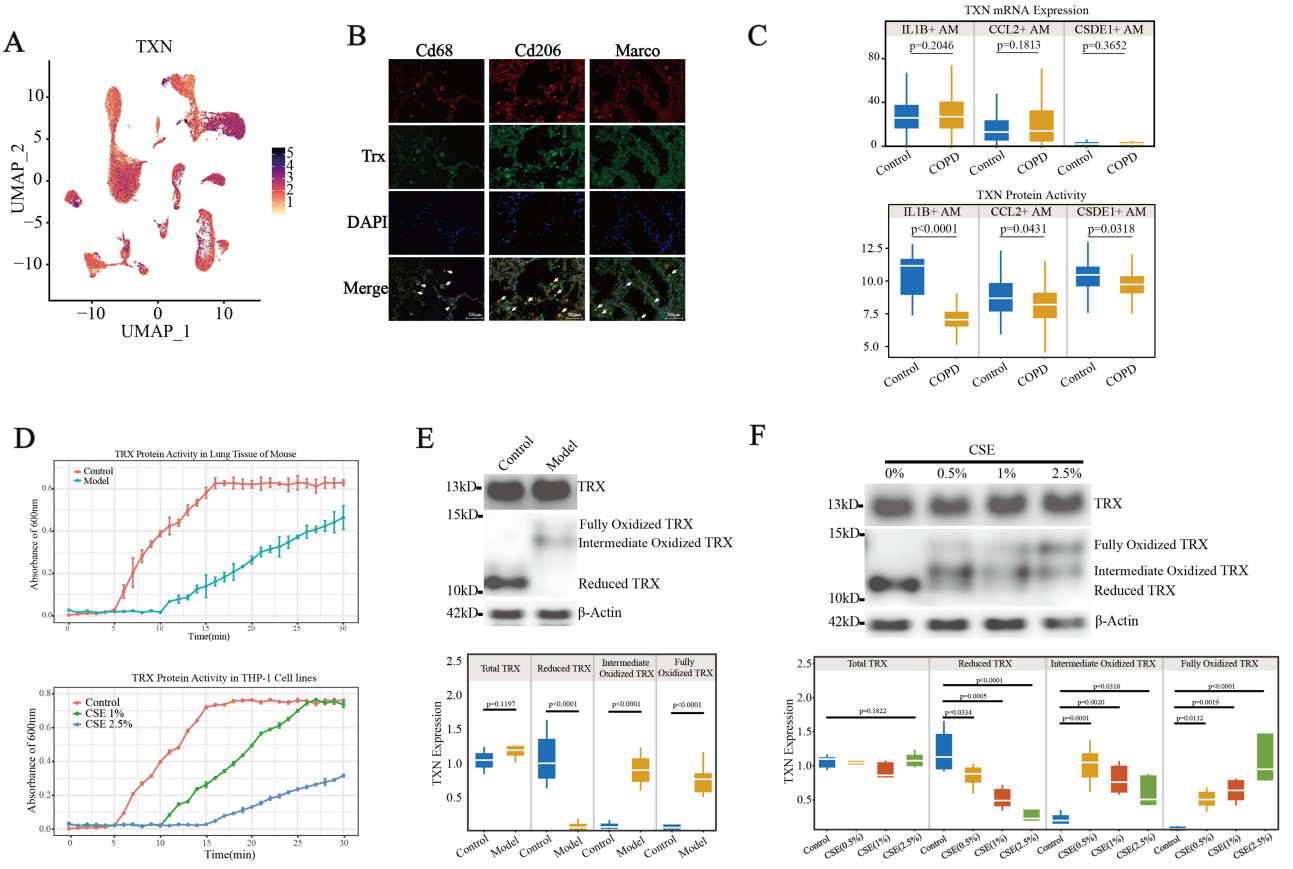

Figure 3 Analysis of changes in TRX activity. (**A**) TRX expression in cellular subclusters UMAP mapping diagram It can be seen that TRX is mainly distributed in AM, pDC and some ciliated epithelial cells. (**B**) Immunofluorescence co-localization TXN can be co-localized with alveolar macrophage markers in mouse lung tissue sections (Arrows indicate co-localized cells). (**C**) Box line plot Demonstration of the mRNA expression and protein activity of TRX in AM. (**D**) Line graphs The upper graph demonstrates TRX activity in lung tissues of mouse model and the lower graph demonstrates TRX activity in THP-1 cell model. (**E** and **F**) Box line plots SDS-PAGE was performed to detect the total TRX content in the mouse model lung tissue and THP-1 model (uppermost band), and NATIVE-PAGE was performed to detect the reduced and non-reduced TRX content in the mouse model lung tissue and THP-1 model (middle band).

 https://doi.org/10.2147/JIR.S513004

electrophoresis (Figure 3E and 3D), and there was no significant change in the total amount of TRX in the model group in the animal model relative to the control group. In the cellular model, there was no significant change in the total amount of TRX as the concentration of CSE increased (Figure 3F). The redox state of TRX in the model was examined using non-denaturing electrophoresis. In the animal model, the amount of reduced TRX decreased and the amount of intermediate and fully oxidized TRX increased in the model group relative to the control group. In the animal model, the amount of reduced TRX gradually decreased with the increase of CSE concentration, intermediate oxidized TRX was highest in the CSE 0.5% group and gradually decreased with the increase of CSE concentration, and the amount of fully oxidized TRX increased with the increase of CSE concentration. Enzyme activity assays and immunoblotting experiments confirmed the accuracy of the scRNA-seq data. TRX, distributed in alveolar macrophages, showed no change in expression in COPD. However, because of elevated oxidative stress in COPD, it resulted in a decrease in reTRX and an increase in oxTRX.

Decreased reTRX in IL-1β+ AM Promotes NLRP3 Activation and IL-1β Release

In addition to its antioxidant activity, TRX also regulates numerous protein activities. We analyzed the results of protein activity prediction (Figure 4A). TRX may be regulated inflammation-related gene such as IL1B, FPR3, IL3RA, LGALS3. IL-1β was specifically expressed in IL-1β+ AM, and in order to confirm whether it is associated with oxidative status of TRX correlation, we performed dot blotting of IL-1β in the supernatant of cell models (Figure 4B, Supplementary Table S1), which showed that the IL1β release capacity of the CSE group was upregulated, and the EC50 of LPS-stimulated IL-1β release from THP-1 was reduced from 15.48 μg/mL to 1.47 μg/mL. The addition of reTXN resulted in the rise of the EC50 to 25.33 μg/mL, which inhibited the IL1β release. And the addition of TXN inhibitor PX12 increased the EC50 to 0.64 μg/mL, which promoted IL-1β release. The addition of oxTXN protein resulted in an EC50 of 2.40 μg/mL, which was close to the CSE group and had no significant effect on IL-1β release capacity. With this experiment, we confirmed that reTRX inhibited IL-1β release, while oxTRX did not inhibit IL-1β release.

IL-1β release is dependent on the activated assembly of inflammasome, and the current study suggests that IL-1β release can be regulated through NLRP1 or NLRP3 in macrophages. To confirm whether TRX regulates IL-1β release through NLRP1 or NLRP3, we performed a pseudo-timing analysis of IL-1β+ AM using Monocle2 (Figure 4C). As pseudo-time classified the cells into 3 states, the percentage of cells in each state gradually increased in COPD. With cell differentiation, the expression of IL-1β and NLRP3 gradually increased, while NLRP1 first increased and then decreased (Figure 4D), and the expression of TRX did not change significantly. The changes in protein activity with cell differentiation were viewed (Figure 4E). It was seen that with pseudo-time changes, TRX activity gradually decreased and the activity of NLRP3 gradually increased.The trend of activity changes of NLRP3 had a stronger correlation than that of NLRP1. The correlation analysis of protein activities (Figure 4F) also confirmed that the activity of NLRP3 gradually decreased with the rise of TRX activity.Therefore, we hypothesized that TRX achieves the regulation of IL-1β production through NLRP3.

To confirm the effect of the reTRX on NLRP3 activity, we performed dot blotting of IL-1β in the supernatant of cell models (Figure 4F). IL-1β release from THP-1 cells was induced using ATP, the endogenous agonist of NLRP3 (Figure 4G, Supplementary Table S1). The EC50 of ATP concentration in the CSE group relative to the control group was reduced from 42.38 μM to 4.43 μM, with upregulation of IL-1β release capacity. The addition of reTXN increased the EC50 to 19.66 μM in the comparison CSE group, inhibiting IL-1β release. After adding the NLRP3 agonist MCC950, the EC50 of the comparative CSE group decreased to 0.57 μM, and the co-intervention with reTRX and MCC950 decreased the EC50 to 4.50 μM compared with reTRX alone. We confirmed that reTRX inhibited IL-1β release, and that the NLRP3 agonist MCC950 mitigated this inhibitory effect. That is, reTRX modulated IL-1β release through NLRP3.

To understand whether oxTRX could modulate NLRP3 activity, we used oxTRX to intervene with THP-1 (Figure 4H, Supplementary Table S1). The EC50 of ATP concentration in the CSE group relative to the control group was reduced from 99.75 μM to 7.31 μM. The addition of oxTRX resulted in a change in the EC50 of the comparative CSE group to 8.41 μM, which did not inhibit IL-1β release. After adding the NLRP3 agonist MCC950, the EC50 decreased to 0.78 μM. Using the co-intervention of oxTRX and MCC950, the EC50 became 1.14 μM. We confirmed that oxTRX did not modulate the release of

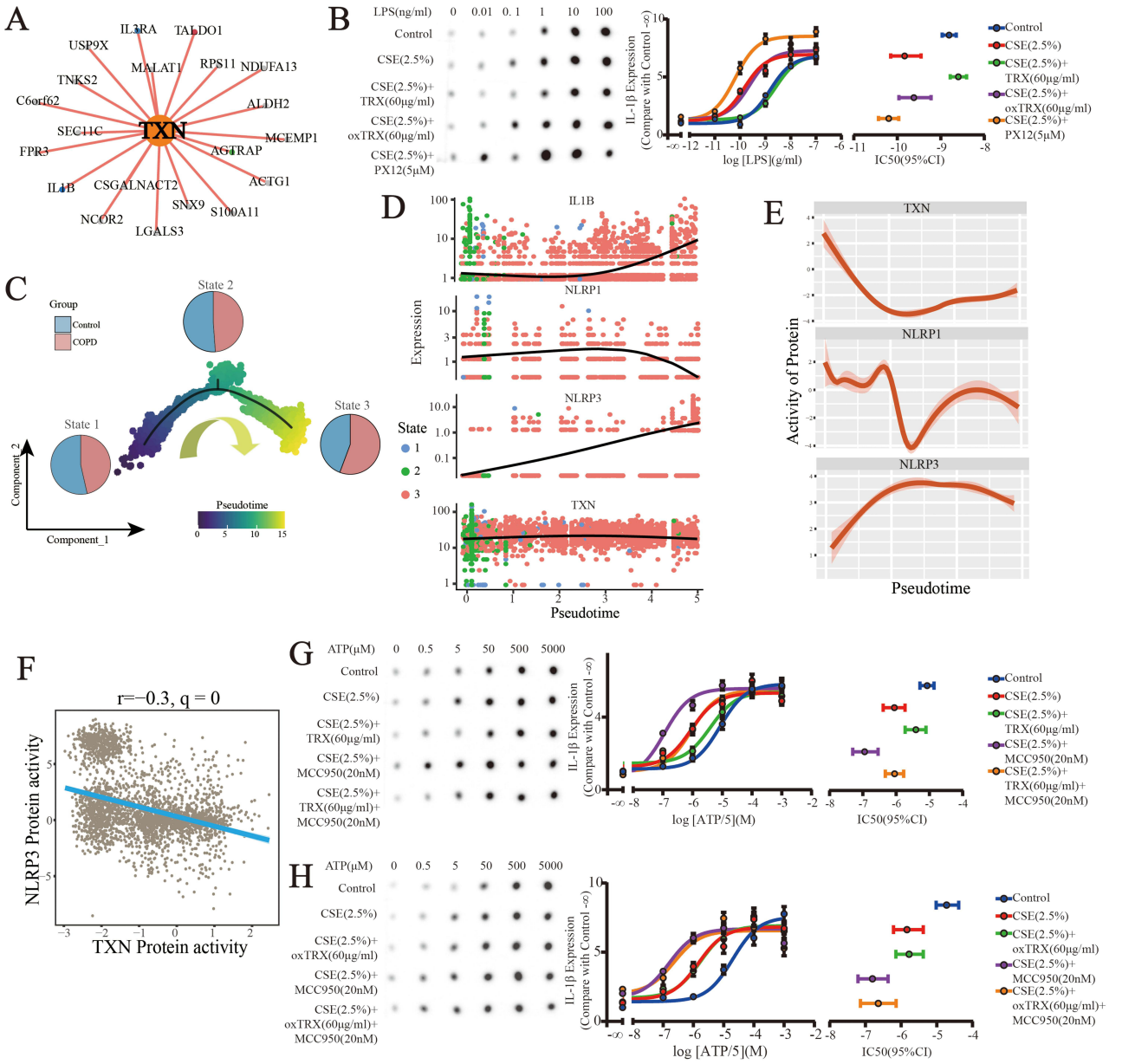

Figure 4 TRX regulates IL-1β release through NLRP3. (**A**) TRX regulated downstream gene. (**B**) The left panel shows the spot blot of supernatant IL-1β in the cell model (n=5), the horizontal axis represents the LPS concentration and the vertical axis represents the treatment group. The middle panel shows the fitted curves, and the relative expression was calculated using Control group LPS 0ng/mL as the reference point. The right panel shows the EC50 of the fitted curves for each group. (**C**) Plot of Monocle2 fitted time series analysis of IL1β+ AM. (**D**) Changes in IL1B, NLRP1, NLRP3, and TXN genes with pseudo-time. (**E**) Changes in NLRP1, NLRP3, and TRX protein activities with pseudo-time. (**F**) Correlation type analysis of TRX activity and NLRP3 activity. (**G** and **H**) The left panel shows speckle blots of supernatant IL-1β in a cell model (n=5), with the horizontal axis representing ATP concentration and the vertical axis representing treatment grouping. The middle panel shows the fitted curves, and the relative expression was calculated using Control group ATP 0 M as the reference point. The right panel shows the EC50 of the fitted curves for each group.

IL-1β through NLRP3. In conclusion, the effect of CSE on IL-1β release from macrophages was due to a decrease in reTRX after CSE stimulation, which promotes NLRP3-regulated IL-1β release, and not due to an increase in oxTRX.

TRX Agonizes NLRP3 by Dissociation TXNIP

TXNIP is an inhibitory protein structural domain protein that binds to TRX and has a role in regulating glucose metabolism, inflammation, and apoptosis.[39] Previous studies suggested that TRX inhibits TXNIP activity by interacting with TXNIP via cysteine C247 to form a complex when the disulfide bond of TRX is in the reduced state. We demonstrated by previous experiments that oxTRX has no regulatory effect on NLRP3 and reTRX inhibits NLRP3

activity. Therefore, it is speculated that when TRX is oxidized, TRX depolymerizes with TXNIP, and then the regulation of NLRP3 is realized. And the activation of NLRP3 may be realized by TXNIP directly interacting with NLRP3, or may be realized by reTRX directly inhibiting NLRP3.[8,13]

In order to clarify how reTRX regulates NLRP3 activity, We need to confirm reTRX and TXNIP who can bind and regulate NLRP3 activity. NLRP3 consists of three structural domains, PYD, NACHT, and LRR (Figure 5A). When the PYD and NACHT structural domains are close to each other, they are in closed conformation (NLRP3_CLOSE), which is in the inactivated state. When the PDY and NACHT domains are far away from each other, they are in the open conformation (NLRP3_OPEN), which is in the activated state.[40] Molecular dynamics simulations were performed by constructing the NLRP3_OPEN/ATP, NLRP3_OPEN/ATP/reTRX, and NLRP3_OPEN/ATP/TXNIP systems (Figure 5B), and the stability of the activation state of NLRP3 was determined by the binding ability between ATP and NLRP3_OPEN. It can be seen that the RMSD value of ATP is highest in the NLRP3/reTRX/ATP system, followed by the NLRP3/ATP system and lowest in the NLRP3/TXNIP/ATP system. This indicates that the binding between ATP, and NLRP3_OPEN is most stable in the system in the presence of TXNIP, whereas the binding between ATP and NLRP3_OPEN is looser in the presence of reTXN. Binding free energy analysis of the interacting amino acids (Figure 5C) showed that TNXIP mainly binds to the NACHT and LRR structural domains, and reTXN mainly binds

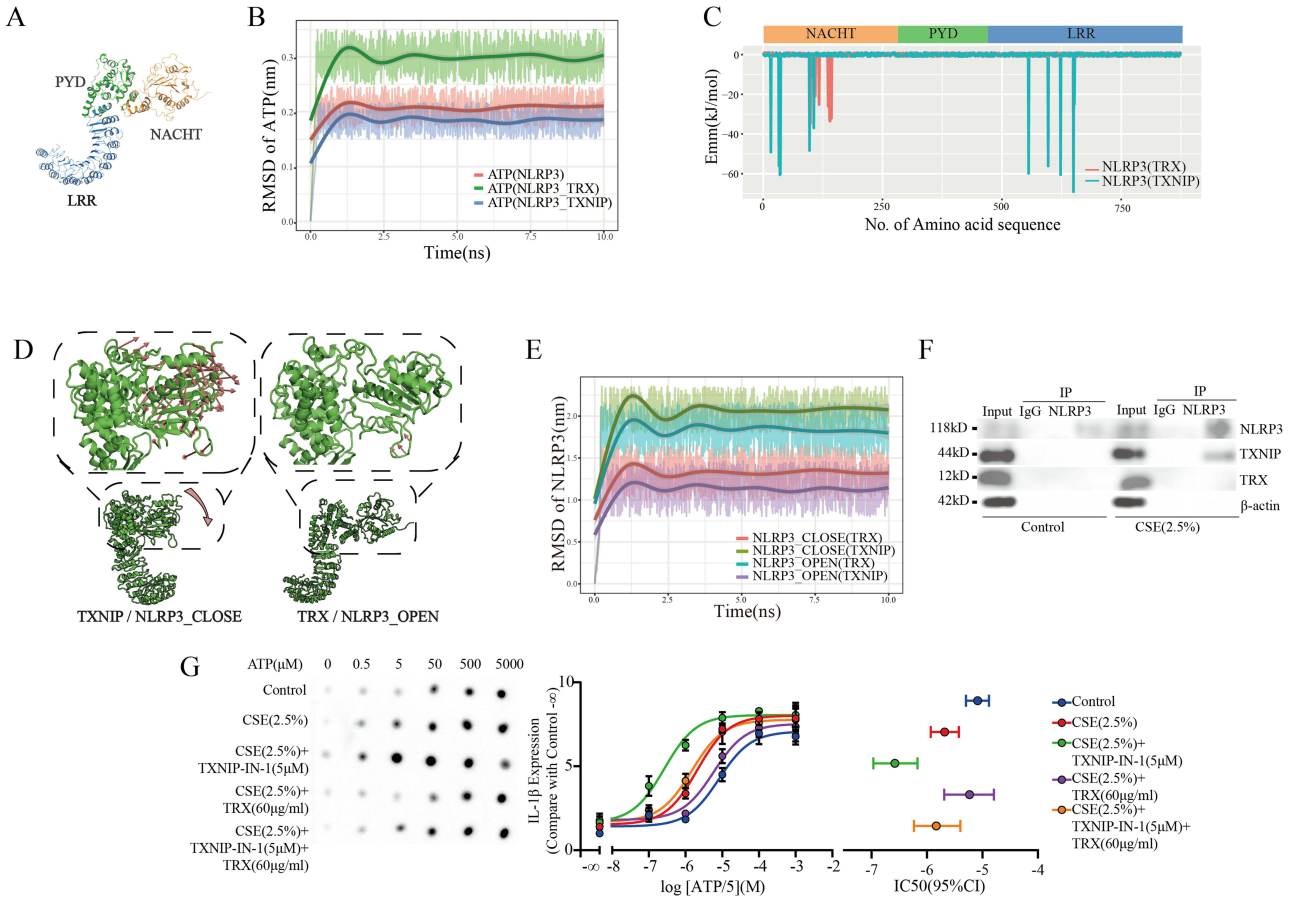

Figure 5 Effect of TRX on NLRP3. (**A**) Three-dimensional structure of NLRP3. (**B**) Degree of deformation for MD The horizontal axis is time and the vertical axis is the RMSD of ATP in the system, in response to calculating the degree of conformational change of the molecule. (**C**) Line graph Calculation of the binding free energy of NLRP3 and TRX, TXNIP, with the amino acid sequence number of NLRP3 on the horizontal axis and the binding free energy (Emm) on the vertical axis. (**D**) Structural changes of NLRP3 in MD The NLRP3_CLOSE conformation bound to TXNIP gradually metastasizes to the NLRP3_OPEN conformation (left); the NLRP3_OPEN conformation bound to TRX gradually metastasizes to the NLRP3_CLOSE conformation (right). (**E**) Degree of deformation for MD The horizontal axis is time and the vertical axis is the RMSD of ATP in the system, and the reaction calculates the degree of conformational change of the molecule. (**F**) CO-IP experiment The control group on the left and the CSE group on the right were subjected to WB detection of proteins by pulling down NLRP3. (**G**) The left panel shows a spot blot of supernatant IL-1β in a cell model (n=5), with the horizontal axis representing ATP concentration and the vertical axis representing treatment grouping. The middle panel shows the fitted curves, and the relative expression was calculated using Control group ATP 0 M as the reference point. The right panel shows the EC50 of the fitted curves for each group.

https://doi.org/10.2147/JIR.S513004

to the NACHT structural domain. The average binding free energy of TXNIP is higher than that of reTRX, which demonstrates that the binding of TXNIP to NLRP3 is more stable than that of reTRX to NLRP3. Referring to the movement trajectory of NLRP3 (Figure 5D), TXNIP binding to NLRP3 pulled apart the NACHT structural domain with the help of LRR, which resulted in a shift from NLRP3_CLOSE conformation to NLRP3_OPEN conformation. Correspondingly, after reTRX bound NLRP3_OPEN, the positions of the NACHT structural domains and PYD structural domains did not change significantly. The NLRP3_OPEN conformation was still maintained, which was inconsistent with the aforementioned experimental results that TRX could inhibit the activity of NLRP3. RMSD analysis showed that the degree of conformational change of NLRP3 in the NLRP3_CLOSE/TXNIP system was greater than that of NLRP3_CLOSE/TRX, while the degree of conformational change of NLRP3 in the NLRP3_OPEN/TXNIP system was less than that of NLRP3_OPEN/TRX (Figure 5E). This suggests that reTRX does not interact with NLRP3. The molecular dynamics simulation results suggest that TRX does not act directly on NLRP3, but dissociates TXNIP after TRX oxidation. Then TXNIP interacts with NLRP3, leading to NLRP3 activation.

To confirm the interaction, we performed CO-IP experiments on cell models (Figure 5F). Whether TRX or TXNIP interacted with NLRP3 was detected by pulling down NLRP3. In the control group, no bound TRX and TXNIP were detected after pulling down NLRP3. In the CSE group, TXNIP was detected but not TRX after pulling down NLRP3. This suggests that TRX does not interact with NLRP3 but exerts its effect through TNXIP interaction with NLRP3 in the THP-1 cell line treated with CSE. We treated THP-1 cell model by the TRX-TXNIP interaction inhibitor TXNIP-IN-1 (Figure 5G, Supplementary Table S1). The EC50 of ATP concentration in the CSE group relative to the control group was reduced from 40.87 μM to 10.39 μM. After the addition of TXNIP-IN-1 decreased the EC50 relative to the CSE group to 1.317 μM, which promoted the IL-1β release. After the addition of reTRX, the EC50 of the relative CSE group increased to 29.35 μM, inhibiting IL-1β release. With the co-intervention of TRX and TXNIP-IN-1, the EC50 became 7.36 μM. It was seen that TXNIP-IN-1 blocked the TRX mediated NLRP3 inhibition.Combining the results of immunoprecipitation and spot blotting, we deduced that TRX was oxidized, TRX and TXNIP dissociated, and TXNIP interacted with and agonized NLRP3, which promoted the release of IL-1β, thus achieving the regulation of NLRP3.

Discussion

COPD is a disease with a complex etiology, including inflammatory response, oxidative stress, tissue damage and abnormal repair. Among them, the inflammatory response as a core pathological mechanism, and oxidative stress promote each other. In lung tissue, different cells exercise different functions. scRNA-seq provides a research tool to understand cellular-level alterations in COPD, revealing the roles played by epithelial cells, lymphocytes, granulocytes, and dendritic cells in the development of COPD disease. AM can modulate lung immune homeostasis by secreting inflammatory factors, such as IL-1β, TNF-α, and IFN-γ, and by exerting nonspecific immune effects through the production of ROS.[41] Cigarette smoke exposure promotes the release of inflammatory factors such as IL-1β and TNF-α from AM, which is an important cause of emphysema in the lungs.[42] Our study identified a subclusters of IL-1β+ AM that specifically expresses IL-1β, and enrichment analysis showed that IL-1β+ AM performs the biological functions of inflammatory response, cytokine release, and production of ROS. IL-1β is mainly secreted by macrophages, and there is a positive correlation between the level of IL-1β secretion and disease severity. This suggests that IL-1β+ AM may play an important role in the development of COPD.

Smoking and air pollution are major triggers of oxidative stress in COPD, and these harmful particulate matter activate ROS generation. Inflammatory factor synthesis and release and ROS production in moderation can help lung tissue to remove stress damage and promote tissue repair, but excessive inflammatory factor synthesis and release and ROS production can exacerbate lung tissue damage and promote disease progression.[41] Counteracting the damage caused by excessive ROS depends on endogenous antioxidant systems such as TRX, GSH and SOD. Previous studies have shown that TRX is expressed in lung tissues in both alveolar macrophages and bronchial epithelial cells, and the overall expression level, although slightly elevated in COPD, did not reach statistical significance. However, in the present study, we found that TRX expression was not increased in the AM subpopulation by scRNA-seq analysis. We further validated this result in a THP-1 cell model, suggesting that there may be cellular-level heterogeneity in TRX changes in lung tissues. In addition, in a mouse model of COPD, we similarly did not observe a significant increase in TRX expression levels, suggesting the heterogeneity of COPD in human

disease and animal models.[43] We report the distribution and redox state changes of TRX in COPD patients for the first time. oxTRX increased and reTRX decreased in IL-1β+ AM in COPD. This explains that although there is no change in TRX levels in COPD, additional provision of reTRX can benefit CSE-induced COPD animal models.[44,45] Combined with numerous previous studies confirming increased ROS in AM, it is hypothesized that the TRX system of AM is protecting the cells from damage by oxidative stress and leading to reTRX depletion.

Oxidative stress can exacerbate disease progression by modulating the inflammatory response through multiple pathways. For example, ROS can activate the synthesis and release of activating cytokines through NF-κB, Nrf2, NLRP3 and other pathways.[46] When supplemented with antioxidant substances, the prognosis of COPD patients or animal models can be improved, but this often requires high doses of antioxidant substances.[47] TRX reduces oxidative damage to proteins and lipids by ROS.[48] It also ameliorates the inflammatory response through processes such as granulocyte apoptosis, cytokine and chemokine release.[49] Here we confirm that CSE induced IL-1β release is associated with a decrease in reTRX and not due to an increase in oxTRX. Instead, reTRX upregulated NLRP3 activity to achieve IL-1β release. Combined with the aforementioned changes in TRX distribution and redox state in COPD, it can be confirmed that oxidative stress causes reTRX to be oxidized to oxTRX in IL-1β+ AM. And the reduction of reTRX upregulates NLRP3 activity and promotes the release of IL-1β.

TXNIP, as an interacting protein of TRX, can regulate each other's activity to affect the oxidative state.TXNIP can inhibit TRX activity by binding to TRX, which can lead to ROS accumulation and induce inflammation or apoptosis. After TRX is oxidized, TXNIP dissociates with TRX. The dissociated TXNIP is activated and produces effects that promote cytokine release, interfere with glucose metabolism, and promote apoptosis.[13,50] TRX inhibits TXNIP activity by binding to TXNIP, which inhibits cytokine release, among other effects. Previous studies suggest that TRX may regulate NLRP3 activity either through direct action on NLRP3 or through TXNIP.[8,13] Here we determined that reTXN was decreased to agonize NLRP3 by depolymerizing TXNIP, which acts on NLRP3, rather than by the effect of reTXN acting directly on NLRP3. Therefore, CSE induced IL-1β release can be improved by increasing reTRX levels.

In conclusion, in this study, we identified a subclusters of AM specifically expressing IL-1β in scRNA-seq. TRX levels specifically distributed to IL-1β+ AM were unchanged, but reTXN was reduced and oxTXN increased. Decreased reTRX led to TXNIP depolymerization, which promotes IL-1β+ AM release in COPD via TXNIP binding to NLRP3. It is suggested that in addition to increasing exogenous TRX, it can also be attempted to improve the redox state of TRX as a way to develop a treatment for COPD. And inhibiting the interaction of TXNIP with NLRP3 might improve IL-1β release due to oxidative stress. While this provides new insights into our understanding of the role played by TRX in COPD, the limitations of this study should also be seen. We validated the scRAN-seq data using a mouse cigarette-induced model and a CSE induced model of the THP-1 cell line, but assays in human lung tissue and human AM primary cell models are still lacking. In addition, we lacked exploration of the upstream of TRX, which could be a future experimental direction for more in-depth exploration of COPD pathomechanisms.

Conclusion

In this study, we analyzed single-cell scRNA-seq data from healthy and COPD lung tissues. A subcluster of AM that specifically expresses IL-1β was identified. In COPD, there was no change in TRX expression of IL-1β+ AM, and the protein activity was decreased, which resulted in a decrease in the antioxidant activity of TRX and a decrease in the ability to inhibit the release of IL-1β from NLRP3. This process helps to explain the role of TRX in the immune-inflammatory response and oxidative stress process in COPD, as well as the pharmacological effects of TRX in the treatment of COPD.

Data Sharing Statement

The data and code in the current study are available from the first author upon reasonable request.

Ethics Statement

The animal experiments involved in this study were approved by the Ethics Committee of Kunming Medical University (kmmu-20221240) in accordance with the Regulations on the Management of Experimental Animals in Yunnan Province and the Measures for the Administration of Experimental Animal Licenses in Yunnan Province.

The human data portion of the study involved in this research was granted exemption from review by the Ethics Committee of Kunming Medical University in accordance with the Measures for Ethical Review of Life Science and Medical Research Involving Human Subjects dated February 18, 2023, China.

Funding

This work was funded by the National Natural Science Foundation of China (No. 81870037, 82160013, 82460012); Science and Technology Program of Yunnan Province (No. 202402AA310007, XDYC-MY-2022-0018, 202201AY070001-073); Kunming Development and Reform Commission (202202); First-Class Discipline Team of Kunming Medical University (2024XKTDTS13); Yunnan Key Laboratory of Pharmacology for Natural Products (YKLPNP-K2403). In addition, this study was supported in part by.

Disclosure

The authors declare no conflicts of interest.

References

1. Kansal H, Chopra V, Garg K, Sharma S. Role of thioredoxin in chronic obstructive pulmonary disease (COPD): a promising future target. *Respir Res*. 2023;24(1):295. doi:10.1186/s12931-023-02574-4
2. Dailah HG. Therapeutic potential of small molecules targeting oxidative stress in the treatment of Chronic Obstructive Pulmonary Disease (COPD): a comprehensive review. *Molecules*. 27(17). doi:10.3390/molecules27175542
3. An N, Kang Y. Thioredoxin and hematologic malignancies. *Adv Cancer Res*. 2014;122:245–279. doi:10.1016/b978-0-12-420117-0.00007-4
4. Modi T, Huihui J, Ghosh K, Ozkan SB. Ancient thioredoxins evolved to modern-day stability-function requirement by altering native state ensemble. *Philos Trans R Soc London Ser B*. 373(1749). doi:10.1098/rstb.2017.0184
5. Kekulandara DN, Nagi S, Seo H, Chow CS, Ahn Y-H. Redox-inactive peptide disrupting Trx1–Ask1 interaction for selective activation of stress signaling. *Biochemistry*. 2018;57(5):772–780. doi:10.1021/acs.biochem.7b01083
6. Zhang X, Lu J, Ren X, et al. Oxidation of structural cysteine residues in thioredoxin 1 by aromatic arsenicals enhances cancer cell cytotoxicity caused by the inhibition of thioredoxin reductase 1. *Free Radic Biol Med*. 2015;89:192–200. doi:10.1016/j.freeradbiomed.2015.07.010
7. Lee S, Kim SM, Lee RT. Thioredoxin and thioredoxin target proteins: from molecular mechanisms to functional significance. *Antioxid Redox Signaling*. 2013;18(10):1165–1207. doi:10.1089/ars.2011.4322
8. Muri J, Thut H, Feng Q, Kopf M. Thioredoxin-1 distinctly promotes NF-κB target DNA binding and NLRP3 inflammasome activation independently of Txnip. *eLife*. 2020;9:e53627. doi:10.7554/eLife.53627
9. Sundaram B, Tweedell RE, Kumar SP, Kanneganti T-D. The NLR family of innate immune and cell death sensors. *Immunity*. 2024;57(4):674–699. doi:10.1016/j.immuni.2024.03.012
10. Xiao C, Cheng S, Li R, et al. Isoforskolin Alleviates AECOPD by improving pulmonary function and attenuating inflammation which involves downregulation of Th17/IL-17A and NF-κB/NLRP3. *Front Pharmacol*. 2021;12:721273. doi:10.3389/fphar.2021.721273
11. Broz P, Dixit VM. Inflammasomes: mechanism of assembly, regulation and signalling. *Nat Rev Immunol*. 2016;16(7):407–420. doi:10.1038/nri.2016.58
12. Ball DP, Tsamouri LP, Wang AE, et al. Oxidized thioredoxin-1 restrains the NLRP1 inflammasome. *Sci Immunol*. 2022;7(77):eabm7200. doi:10.1126/sciimmunol.abm7200
13. Kim W-I, Pak S-W, Lee S-J, et al. Copper oxide nanoparticles exacerbate chronic obstructive pulmonary disease by activating the TXNIP-NLRP3 signaling pathway. *Particle Fibre Toxicology*. 2024;21(1):46. doi:10.1186/s12989-024-00608-3
14. Satija R, Farrell JA, Gennert D, Schier AF, Regev A. Spatial reconstruction of single-cell gene expression data. *Nature Biotechnol*. 2015;33(5):495–502. doi:10.1038/nbt.3192
15. Korsunsky I, Millard N, Fan J, et al. Fast, sensitive and accurate integration of single-cell data with Harmony. *Nature Methods*. 2019;16(12):1289–1296. doi:10.1038/s41592-019-0619-0
16. Germain P-L, Lun A, Meixide CG, Macnair W, Robinson MD. Doublet identification in single-cell sequencing data using scDblFinder. *f1000research*. 2022;10:979. doi:10.12688/f1000research.73600.2
17. Yu G, Wang L-G, Han Y, He Q-Y. clusterProfiler: an R package for comparing biological themes among gene clusters. *OMICS*. 2012;16(5):284–287. doi:10.1089/omi.2011.0118
18. Obradovic A, Chowdhury N, Haake SM, et al. Single-cell protein activity analysis identifies recurrence-associated renal tumor macrophages. *Cell*. 2021;184(11):2988–3005.e16. doi:10.1016/j.cell.2021.04.038
19. Qiu X, Mao Q, Tang Y, et al. Reversed graph embedding resolves complex single-cell trajectories. *Nature Methods*. 2017;14(10):979–982. doi:10.1038/nmeth.4402
20. Ghorani V, Boskabady MH, Khazdair MR, et al. Experimental animal models for COPD: a methodological review[J]. *Tob Induc Dis*. 2017;15(1):25. doi:10.1186/s12971-017-0130-2

21. Jo S, Kim T, Iyer VG, Im W. CHARMM-GUI: a web-based graphical user interface for CHARMM. *J Comput Chem*. 2008;29(11):1859–1865. doi:10.1002/jcc.20945
22. Van Der Spoel D, Lindahl E, Hess B, Groenhof G, Mark AE, Berendsen HJ. GROMACS: fast, flexible, and free. *J Comput Chem*. 2005;26 (16):1701–1718. doi:10.1002/jcc.20291
23. Ms V-T, Me V-T, Valiente PA, Moreno E. gmx_MMPBSA: a new tool to perform end-state free energy calculations with GROMACS. *J Chem Theory Computation*. 2021;17(10):6281–6291. doi:10.1021/acs.jctc.1c00645
24. Barnes P, Celli B. Systemic manifestations and comorbidities of COPD. *Eur Respir J*. 2009;33(5):1165–1185. doi:10.1183/09031936.00128008
25. Brusselle GG, Joos GF, Bracke KR. New insights into the immunology of chronic obstructive pulmonary disease. *Lancet*. 2011;378 (9795):1015–1026. doi:10.1016/S0140-6736(11)60988-4
26. Jamieson T, Cook DN, Nibbs RJ, et al. The chemokine receptor D6 limits the inflammatory response in vivo. *Nat Immunol*. 2005;6(4):403–411. doi:10.1038/ni1182
27. Wang C, Zhou J, Wang J, et al. Progress in the mechanism and targeted drug therapy for COPD. *Signal Trans Targeted Ther*. 2020;5(1):248. doi:10.1038/s41392-020-00345-x
28. Perrot C, Karampitsakos T, Unterman A, et al. MCEMP1 is expressed in classical monocytes and alveolar macrophages in IPF and regulates cell chemotaxis, adhesion, and migration in a TGFβ dependent manner. *Am J Physiol Cell Physiol*. 2024;326:C964–C977. doi:10.1152/ajpcell.00563.2023
29. Zhang Q, Jia Y, Pan P, et al. α5-nAChR associated with Ly6E modulates cell migration via TGF-β1/Smad signaling in non-small cell lung cancer. *Carcinogenesis*. 2022;43(4):393–404. doi:10.1093/carcin/bgac003
30. Wang L, Chen Q, Yu Q, Xiao J, Zhao H. TREM-1 aggravates chronic obstructive pulmonary disease development via activation NLRP3 inflammasome-mediated pyroptosis. *Inflammation Res*. 2021;70(9):971–980. doi:10.1007/s00011-021-01490-x
31. Deshmane SL, Kremlev S, Amini S, Sawaya BE. Monocyte chemoattractant protein-1 (MCP-1): an overview. *J Interferon Cytokine Res*. 2009;29 (6):313–326. doi:10.1089/jir.2008.0027
32. Nucera F, Hansbro PM, Paudel KR, et al. Role of autoimmunity in the pathogenesis of chronic obstructive pulmonary disease and pulmonary emphysema. *Trans Autoimmunity Elsevier*. 2022:311–331.
33. Takiguchi H, Yang Y, Yang C, et al. Gene expression signature of human alveolar macrophages recovered from human broncho-alveolar lavage. *C108 OMICS of COPD and IPF*. 2020;A6128–A6128.
34. Breau M, Marcos E, Tran Van Nhieu J, et al. JunD protects mice from age-related lung alterations consisting of emphysema, lymphoid hyperplasia, and adenocarcinoma. *A70 GOOD the BAD, UGLY AGING*. 2016;A2323–A2323.
35. Veerapaneni U VV, Thimraj S, Thimraj TA, et al. Circulating secretoglobin family 1A member 1 (SCGB1A1) levels as a marker of biomass smoke induced chronic obstructive pulmonary disease. *Toxics*. 2021;9(9):208. doi:10.3390/toxics9090208
36. Alkyoon FAA, Dananah FM. The correlation between serum levels of progranulin and inflammatory markers in patients with chronic obstructive pulmonary disease. *Kufa Med J*. 2024;20(1):90–96. doi:10.36330/kmj.v20i1.15052
37. Caramori G, Casolari P, Barczyk A, Durham AL, Di stefano A, Adcock I. COPD immunopathology. *Springer*. 2016:497–515.
38. Tang D, Kang R. Sqstm1 is a therapeutic target for infection and sterile inflammation. *Cytokine*. 2023;169:156317. doi:10.1016/j.cyto.2023.156317
39. Dagdeviren S, Lee RT, Wu N. Physiological and pathophysiological roles of thioredoxin interacting protein: a perspective on redox inflammation and metabolism. *Antioxid Redox Signaling*. 2023;38(4):442–460. doi:10.1089/ars.2022.0022
40. Yu X, Matico RE, Miller R, et al. Structural basis for the oligomerization-facilitated NLRP3 activation. *Nat Commun*. 2024;15(1):1164. doi:10.1038/s41467-024-45396-8
41. Lugg ST, Scott A, Parekh D, Naidu B, Thickett DR. Cigarette smoke exposure and alveolar macrophages: mechanisms for lung disease. *Thorax*. 2022;77(1):94–101. doi:10.1136/thoraxjnl-2020-216296
42. Alexander LEC, Shin S, Hwang JH. Inflammatory diseases of the lung induced by conventional cigarette smoke: a review. *Chest*. 2015;148 (5):1307–1322. doi:10.1378/chest.15-0409
43. Lehtonen ST, Ohlmeier S, Kaarteenaho-Wiik R, et al. Does the oxidative stress in chronic obstructive pulmonary disease cause thioredoxin/peroxiredoxin oxidation? *Antioxid Redox Signaling*. 2008;10(4):813–820. doi:10.1089/ars.2007.1952
44. Sato A, Hoshino Y, Hara T, et al. Thioredoxin-1 ameliorates cigarette smoke-induced lung inflammation and emphysema in mice. *J Pharmacol Exp Ther*. 2008;325(2):380–388. doi:10.1124/jpet.107.134007
45. Hoshino Y, Nakamura T, Sato A, Mishima M, Yodoi J, Nakamura H. Neurotropin demonstrates cytoprotective effects in lung cells through the induction of thioredoxin-1. *Am J Respir Cell Mol Biol*. 2007;37(4):438–446. doi:10.1165/rcmb.2006-0402OC
46. Hikichi M, Mizumura K, Maruoka S, Gon Y. Pathogenesis of chronic obstructive pulmonary disease (COPD) induced by cigarette smoke. *J Thoracic Dis*. 2019;11(Suppl 17):S2129. doi:10.21037/jtd.2019.10.43
47. Vlahos R, Bozinovski S. Glutathione peroxidase-1 as a novel therapeutic target for COPD. *Redox Rep*. 2013;18(4):142–149. doi:10.1179/1351000213Y.0000000053
48. Aoyama K, Nakaki T. Glutathione in cellular redox homeostasis: association with the excitatory amino acid carrier 1 (EAAC1). *Molecules*. 2015;20 (5):8742–8758. doi:10.3390/molecules20058742
49. Ruan Z, Liu G, Guo Y, et al. First report of a thioredoxin homologue in jellyfish: molecular cloning, expression and antioxidant activity of CcTrx1 from Cyanea capillata. *PLoS One*. 2014;9(5):e97509. doi:10.1371/journal.pone.0097509
50. Pan M, Zhang F, Qu K, Liu C, Zhang J. TXNIP: a double-edged sword in disease and therapeutic outlook. *Oxid Med Cell Longev*. 2022;2022 (1):7805115. doi:10.1155/2022/7805115